URSI - RCRS 2022, IIT (Indore), India, 1 - 4 December, 2022

Point Source Carbon Dioxide Emission Monitoring Using Radiative Transfer Simulations and AVIRIS-NG Data

Hasmukh K. Varchand* (1), Mehul R. Pandya (2), Jalpesh A. Dave (1), Parthkumar N. Parmar (1), Himanshu J. Trivedi (1)
(1) N. V. Patel College of Pure and Applied Sciences, Vallabh Vidyanagar, Gujarat, India.
(2) Space Applications Center, Indian Space Research Organisation, Ahmedabad, Gujarat, India.

Abstract

The significant amount of Carbon Dioxide (CO_2) emission causes radiative forcing in the atmosphere that increases the earth's temperature. To reduce the emission from anthropogenic activity, it is important to monitor the major sources and sinks of atmospheric CO_2 such as coal-fired Thermal Power Plant (TPP). Airborne hyperspectral sensors with contiguous spectral bands have capabilities to measure point source CO_2 emission. In this study, we have estimated CO_2 concentration using Radiative Transfer (RT) simulations and Airborne Visible/InfraRed Imaging Spectrometer - Next Generation (AVIRIS-NG) data acquired on Maithon TPP at Jharkhand in India. Due to its higher sensitivity to the boundary layer atmosphere, the Short-Wave InfraRed (SWIR) region is most suitable for the detection of CO_2 emission sources. we used a 2.0 µm absorption band for CO_2 plum detection. This paper describes the Continuum Interpolated Band Ratio (CIBR) method for measurement of CO_2 concentration in the atmosphere which is emitted by TPP.

Index Terms – CO_2, Thermal Power Plant, SWIR, AVIRIS-NG, Radiative Transfer.

1. Introduction

CO_2 absorbs solar radiation that increases the atmospheric temperature, further it causes climate warming by radiative forcing. Coal-fired TPP is a significant source of anthropogenic CO_2 emission that can increase CO_2 concentration in the atmosphere through coal-burning activities [1]. The thermal power sector in India, emits 1.1 gigatonnes of CO_2 every year. it contributes to 2.5% of global Greenhouse Gas (GHG) emissions and one-third of India's GHG emissions. nearly half of India's fuel-related CO_2 emissions come up from TPP. [2]. Reducing the emission from TPP needs better estimation by accurate measurement techniques, which should be affordable and easily available on a global scale. Mostly in developed countries, TPPs are equipped with continuous emission monitoring systems (CEMS) that directly measure CO_2 emission within the stack. However, CEMS equipment is expensive and needs frequent calibration [3]. Hyperspectral sensors with higher spectral and spatial resolution have the potential to estimate point source CO_2 emission. The RT model is used to theoretical measurement of CO_2 concentration within pixels of scenes that are further used to generate the band ratio method. Many hyperspectral sensors have been developed for CO_2 detection such as SCanning Imaging Absorption spectroMeter for Atmospheric CartograpHY (SCIAMACHY) provides the global measurement of various trace gases in the atmosphere like CO_2 and Methane (CH_4) [4]. Greenhouse Gas Observation SATellite (GOSAT) carrying Thermal And Near infrared Sensor for carbon Observation Fourier-Transform Spectrometer (TANSO-FTS) is capable to measure CO_2 and CH_4. [5]. NASA's Orbiting Carbon Observatory-2 (OCO-2) is a space-borne instrument with a higher spectral and temporal resolution that measures dry air column CO_2 abundance in weak (1.61 µm) and strong (2.09 µm) absorption bands [6]. OCO-3 is an improved version of OCO-2 with similar specifications and provides information from 2019. The advantage of Snapshot Area Map (SAM) mode in OCO-3 can measure point source CO_2 emission at facility scale such as TPP [7]. Airborne imaging spectrometers like AVIRIS and next generation instrument AVIRIS-NG can map large regions while providing the spatial resolution required to identify point source emission of CO_2 and CH_4 within the scenes [8]. PRISMA (PRecursore IperSpettrale della Missione Applicativa) is also proved to be suitable for trace gas concentration retrieval from space [9]. The objective of this study is to test the CIBR method on hyperspectral sensors to estimate TPP-emitted CO_2.

2. Theory

The availability of CO_2 absorption channels in the satellite sensors provide facility for the measurement of GHG column contents. The strength of absorption in specific spectral bands directly depends on the amount of gas in a column. It means a higher concentration of gas can lead to higher absorption in the wavebands. Measuring absorption in the band can give CO_2 concentration values in the atmosphere. As shown in Figure-1, CO_2 absorption occurs in 1.6 µm (weak) and 2.0 µm (strong) bands in the SWIR region. In these bands, the 2.0 µm band is extensively used for CO_2 retrieval. P. Prasad et. al., (2013) [10] theoretically explains the suitability of the 1.6 µm band for CO_2 concentration retrieval. However, it is not

used here due to lower sensitivity to CO_2. 2.0 µm band is a highly sensitive band in the SWIR region that is commonly used in sensors for point source emission detection. Although it is partially affected by Water Vapor (WV), which may lead to errors in accurate estimation. Many methods have been developed using this band such as Joint Reflectance and Gas Estimator (JRGE) proven effective for CO_2 retrieval in an unknown surface reflectance [11]; Cluster Tunned Matched Filter (CTMF) measures fainted emissions of CO_2 and CH_4 [12]; The CIBR method has been tested for thermal power plant emitted CO_2 detection using 2.0 µm band by M R. Pandya et. al., (2021) [13]. We used the CIBR method in the 2.0 µm absorption band due to its simplicity and higher efficiency.

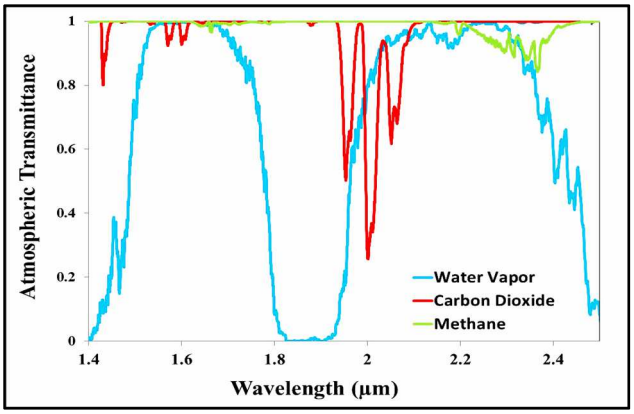

Figure 1: Atmospheric Transmittance curve for the three major GHG (CO_2, WV, and CH_4) in SWIR region (1.4-2.5 µm) generated by MODTRAN simulations.

3. Methodology

3.1. Data and site

The AVIRIS-NG is a push-broom hyperspectral sensor with a broad (380-2500 nm) spectral range and 5 nm spectral resolution. AVIRIS-NG data available from 2018 by the ISRO-NASA joint venture are used here [14]. Level-1 radiance data with nearly 425 contiguous spectral channels, sun-sensor geometry, geo-location, and altitude of flight have been carried out for this study. Coal-based TPP is an ideal location for carrying out surveys using AVIRIS-NG. We have selected Maithon thermal power plant as the study site which is located on the east side of Jharkhand state in the Dhanbad district. For the validation of our work, we utilize wind data from NASA's POWER API database which is open access with long-term coverage [15]. Wind speed at 10 m above ground and direction in degree clockwise from due north at the time and date for AVIRIS-NG flight have been collected from the SSE- Renewable Energy Community of The POWER Data Access Viewer and utilized for the power plant site.

3.2. RT Simulations

MODTRAN (MODerate spectral resolution atmospheric TRANsmittance) model is based on the RT equation which has a 1 cm^{-1} finer spectral resolution [16]. MODTRAN calculates the Top Of Atmosphere (TOA) radiance from earth-emitted radiance, reflected downwelling radiance, and atmospheric path radiance. It is also useful for determining the sensitivity of atmospheric gases such as WV, CO_2, and CH_4. Here we used the MODTRAN RT model to evaluate of sensitivity of CO_2 in the SWIR region. Simulations have been carried out for varying WV concentrations from 0.5 to 4.0 g/cm^2 with a 0.5 gm/cm^2 interval. For each value of WV, CO_2 values have been varying from 200 to 800 ppmv to decouple the effect of WV on CO_2 absorption bands. the change in At-sensor radiance with CO_2 values Generated from the simulation process is shown in figure 2.

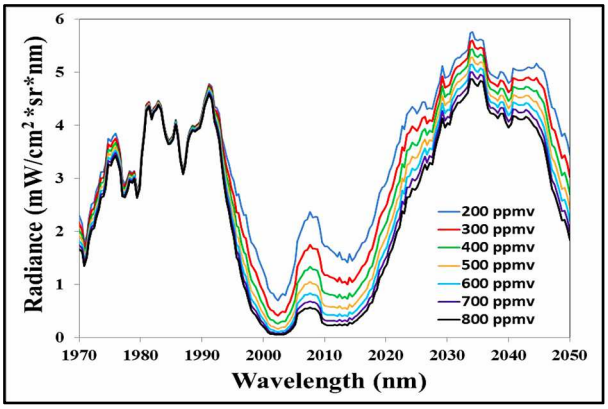

Figure 2: Radiance as function of wavelength for varying values of CO_2 concentrations in 2 µm spectral band generated using MODTRAN RT model (WV- 2.0 g/cm^2).

According to the locations of the power plant, we used a tropical model atmosphere, a standard atmospheric profile and rural aerosol with 23 km visibility has been considered. Other inputs such as solar zenith and azimuth angle, altitude, date, and coordinates of the plant are taken from AVIRIS-NG flight details. 1400 – 2500 nm range considered for AVIRIS-NG SWIR region. The method to decouple the effect of WV in CO_2 absorption bands developed by M.R. Pandya et. al. (2021) [13] has been used here.

3.3. Concentration Retrieval Algorithm

In the CIBR equation, the numerator represents radiance measured by the sensor at the center of the absorption band (L_{min}) which is more affected by the absorption of CO_2, and the denominator represents the sum of wavelength weighted radiances of the two nearest non-absorption bands (L_1 and L_2) which are free from any gas's absorption.

$$CIBR = \frac{L_{min}(\lambda_m)}{f_1 * L_1(\lambda_1) + f_2 * L_2(\lambda_2)} \qquad (1).$$

Here, f_1 and f_2 are weighting coefficients which can be calculated by following equations,

$$f_1 = \frac{\lambda_2 - \lambda_m}{\lambda_2 - \lambda_1} \quad \text{and} \quad f_2 = \frac{\lambda_m - \lambda_1}{\lambda_2 - \lambda_1} \qquad (2).$$

Eq. (1) is applied on a 2.0 µm absorption channel. In this absorption band, λ_m = 2009 nm, λ_1 = 1984 nm and λ_2 = 2034 nm selected and the sum of f_1 and f_2 is always equals

to 1 (f_1+f_2 = 1). The conversion of the CIBR index to CO_2 content in ppmv is done by fitting the curve and generating appropriate curve fitting coefficients. For that, the inversion equation is used as follows,

$$XCO_2 = a * (CIBR^{-b}) + c \quad (3).$$

Where, XCO_2 is the unknown carbon dioxide columnar abundance (ppmv) and a, b and c are the parameters related to the model variables and depends on WV concentration. CO_2 vs. CIBR curve is shown in figure 3. Using these equations, we can calculate CO_2 concentration in all pixels from any observations with known spectral information.

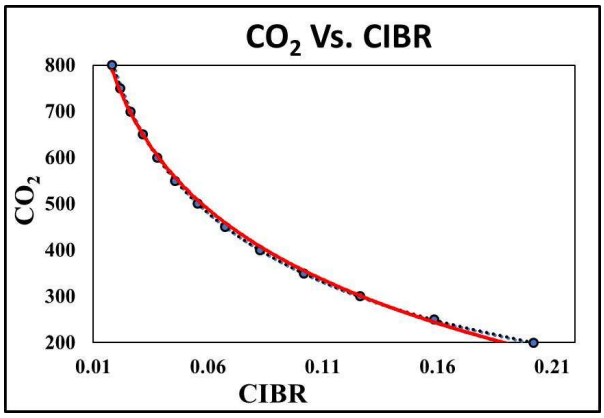

Figure 3: CO_2 vs. CIBR curve generated from MODTRAN simulations to calculate curve fitting parameters.

4. Results

The conversion from CIBR values to XCO_2 estimation is a crucial point. Due to the partial WV effect on this band, CIBR values are changed according to WV concentration in a scene. To remove the WV effect, we generated curve fitting coefficients for different values of WV. After retrieval of CO_2 values and fitting the curve in simulation data for each value of WV, we applied it to the study sites as shown in Figure 4.

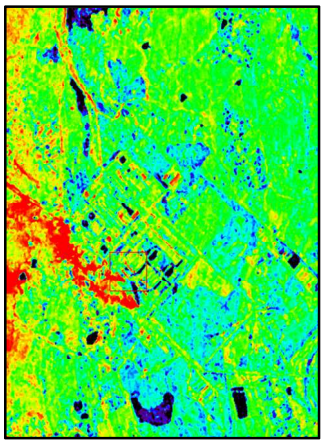

Figure 4: CIBR method tested on Maithon power plant for plum detection.

Here the CIBR shows promising results as the plum is clearly visible and separated from ground reflectance. A graphical interpolation has been applied to AVIRIS-NG data for the enhancement to the plum pixels. Gaussian enhancement and median filters have been applied to overcome the background errors and remove false positive points. Red pixels represent CO_2 values with a maximum of 430 ppmv for the Maithon plant as shown in Figure 5.

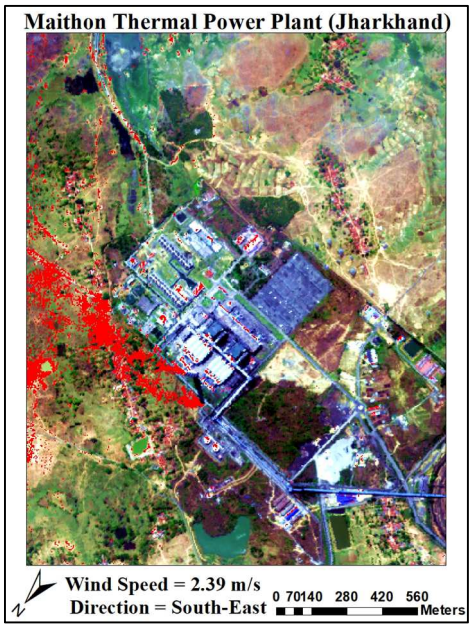

Figure 5: XCO_2 maps from plume detected in real AVIRIS-NG image acquired at Maithon TPP.

Results show that CIBR is a suitable method for CO_2 detection using the SWIR spectral band. The direction of the wind at the acquisition matches the plum direction which indicates the validity of the results. The Maithon site has an intense wind speed of 2.39 m/s on the east-south side showing more expansion of plum. Comparisons of results with AVIRIS-NG benchmark datasets for CO_2 retrieval at the Maithon site show similar results [17].

5. Conclusions

In this study, we investigated the potential of the AVIRIS-NG hyperspectral mission to map CO_2 plum emitted from coal-based TPP. The SWIR spectral range shows adequate results for CO_2 retrievals with high sensitivity and low errors of other parameters which makes it suitable for CO_2 emission sources detection. Our study shows the capabilities of the CIBR method to monitor point source CO_2 emission. This method gives accurate CO_2 plum detection originating from coal burning activities. Remote sensing methods for the estimation of CO_2 emissions are cheaper than standard emission monitoring methods. It does not need continuous calibration and hence eliminates measurement errors. Also, this type of method can be applicable to large areas and any part of the country, which is never possible in

standard emission measurement instruments which are mounted within the facility. Continuous monitoring gives the right information about the health of the power plant and used fuel. It is useful to make decisions to overcome CO_2 emissions from the point sources and make policies to reduce atmospheric pollution to improve air quality. This method gives promising results to estimate power plant emissions. In the future, our aim is to apply the retrieval method to all Indian power plants using PRISMA satellite data to estimate CO_2 emissions.

6. Acknowledgements

The authors would like to thank the Director, SAC-ISRO and Principal NVPAS for the encouragement and support to this study. We would like to extend our gratitude to the Gujarat government for providing the SHODH (ScHeme Of Developing High quality research) scholarship as financial support. Authors would acknowledge ISRO and JPL – NASA team for providing AVIRIS-NG data.

7. References

1. P. Ciais, A. J. Dolman, A. Bombelli, R. Duren, A. Peregon, P. J. Miller et. al., "Current systematic carbon-cycle observations and the need for implementing a policy-relevant carbon observing system," Biogeosciences, **11**, 13, pp. 3547–3602, 2014, doi: 10.5194/bg-11-3547-2014.
2. N. K. Yadav, S. Kannappan, S. Ramanathan and S. Arora, "Perform, Achieve and Trade (PAT) Scheme in TPP: A Critical Analysis," Centre for Science and Environment, New Delhi, 2021.
3. K. Gurney, R. Huang, and K. Coltin, "Bias present in US federal agency power plant CO2 emissions data and implications for the US clean power plant," Environmental Research Letters, **11**, 6, pp. 064005, 2016, doi: 10.1088/1748-9326/11/6/064005.
4. G. G. Abad, A. H. Souri, J. Bak, K. Chance, L. E. Flynn, A. K. Nickolay et. al., "Five decades observing Earth's atmospheric trace gases using ultraviolet and visible backscatter solar radiation from space," Journal of Quantitative Spectroscopy and Radiative Transfer, **238**, 106478, 2019, ISSN 0022-4073.
5. A. Kuze, H. Suto, M. Nakajima and T. Hamazaki, "Thermal and near infrared sensor for carbon observation Fourier-transform spectrometer on the GHG Observing Satellite for GHG monitoring," Appl. Opt., **48**, 35, pp. 6716-6733, 2009, doi: 10.1364/AO.48.006716.
6. D. Crisp, "Measuring Atmospheric Carbon Dioxide from the NASA Orbiting Carbon Observatory-2 (OCO-2)," Light, energy and environment 2018 (E2, FTS, HISE, SOLAR, SSL), OSA Technical Digest (Optical Publishing Group, 2018), pp. JT1A.2, 2018, doi: 10.1364/FTS.2018.JT1A.2.
7. M. Kiel, A. Eldering, D. D. Roten, C. John, S. Feng, R. Lei et. al, "Urban-focused satellite CO2 observations from the Orbiting Carbon Observatory-3: A first look at the Los Angeles megacity," Remote Sensing of Environment, **258**, 2021, 112314, ISSN:0034-4257, doi: 10.1016/j.rse.2021.112314.
8. A. K. Thorpe, C. Frenkenberg, D. Thompson, M. R. Duren, A. D. Aubrey et. al., "Airborne DOAS retrievals of methane, carbon dioxide, and water vapor concentrations at high spatial resolution: application to AVIRIS-NG," Atmos. Meas. Tech., **10**, 10, pp. 3833–3850, 2017, doi: 10.5194/amt-10-3833-2017.
9. R. Vito, C. Spinetti, M. Silvestri, and M. F. Buongiorno, "A Methodology for CO2 Retrieval Applied to Hyperspectral PRISMA Data," Remote Sensing, **13**, 22, pp. 4502, 2021. doi: 10.3390/rs13224502.
10. P. Prasad, S. Rastogi, R. P. Singh and S. Panigrahy, "Spectral modelling near the 1.6 μm window for satellite based estimation of CO2," Spectrochim Acta A Mol Biomol Spectrosc, Epub 2013 Aug 19. PMID: 23998965, 117:330-9, Jan. 2014, doi: 10.1016/j.saa.2013.08.035.
11. R. Marion, R. Michel and C. Faye, "Measuring trace gases in plumes from hyperspectral remotely sensed data," in IEEE Transactions on Geoscience and Remote Sensing, **42**, 4, pp. 854-864, April 2004, doi: 10.1109/TGRS.2003.820604.
12. A. K. Thorpe, D. A. Roberts, E. S. Bradley, C. C. Funk, P. E. Dennison, and I. Leifer, "High resolution mapping of methane emissions from marine and terrestrial sources using a Cluster-Tuned Matched Filter technique and imaging spectrometry," Remote Sensing of Environment, **134**, pp. 305-318, 2013, doi: 10.1016/j.rse.2013.03.018.
13. M. R. Pandya, A. Chhabra, V. N. Pathak, H. J. Trivedi, and P. Chauhan, "Mapping of thermal power plant emitted atmospheric carbon dioxide concentration using AVIRIS-NG data and atmospheric RT model simulations," Journal of Applied Remote Sensing, **15**, 3, pp. 032204, 21 April 2021, doi: 10.1117/1.JRS.15.032204.
14. AVIRIS-NG Data Product Portal 2014-2021, Jet Propulsion Laboratory, NASA, Available: https://avirisng.jpl.nasa.gov/dataportal/.
15. Prediction Of Worldwide Energy Resource (POWER) Data Access Viewer, NASA Earth Science/Applied Science Program, Available: https://power.larc.nasa.gov/data-access-viewer/
16. A. Berk, P. Conforti, R. Kennett, T. Perkins, F. Hawes, and J. van den Bosch, "MODTRAN 6: A major upgrade of the MODTRAN® radiative transfer code," 2014 6th Workshop on Hyperspectral Image and Signal Processing: Evolution in Remote Sensing (WHISPERS), pp. 1-4, 2014, doi: 10.1109/WHISPERS.2014.8077573.
17. Benchmark Dataset for Methane and Carbon Dioxide Plumes, Airborne Visible-Infrared Imaging Spectrometer - Next Generation (AVIRIS-NG), JPL-NASA, 2020, Available: https://avirisng.jpl.nasa.gov/benchmark_methane_carbon_dioxide.html.